Journal of Mechanical Engineering Research and Developments
ISSN: 1024-1752
CODEN: JERDFO
Vol.43, No.5, pp. 355-372
Published Year 2020

Thermal Performance Improvement of Double Pass Solar Air Heater

Ameer Resen Kalash, Sameera Sadey Shijer, Laith Jaafer Habeeb

University of Technology / Training and Workshop Center

*Corresponding Author Email: 11171@uotechnology.edu.iq, ssdy88868@gmail.com, 20021@uotechnology.edu.iq

ABSTRACT: The performance of the double pass solar air heater has been investigated experimentally and numerically using computational fluid dynamics. In the experimental investigations, three double pass solar air heaters were fabricated using ten tubes of aluminum. Aluminum Glass wool was used to insulate the sides and the bottom base with a thickness of 25 mm. Three configurations types was used for the experiments. The experiments time lasted through all the light of the day. For the numerical investigations, SolidWorks was used to generate the geometry of the model and Ansys Fluent was used for the simulations. The results showed that the temperature and the solar flux start to increase as the time raises form the morning then start to decrease at noon. Constantly the stored energy increases by day and decreasing by night. It was also found that vortices were generated in the collector by the air velocity.

KEYWORDS: Solar air collector, Numerical simulation for air collector, Solar flux of air collector, Energy storing

INTRODUCTION

Flat-plate collectors usually used for devices that demanding energy transfer at reasonable temperatures; reach to maybe 100◦C overhead ambient temperature. They use both diffuse and beam sun radiation, do not need chasing of the sun, and requests few repairs. As a mechanic, they are simpler than concentrating collectors. The main devices of these items are in solar water heating, air conditioning, industrial process heat, and building heating. Heated buildings can be seen as unusual cases of flat-plate collectors with the room or storage wall as the absorber. Sustainable energy technologies are suitable for a cheerful energy future. These technologies confirm that the supply of energy will continues. The solution for energy crisis in the world depending on effective use of energy, conversion and storage of sustainable energy [1-2]. Researchers always looking up for effectual use of energy. Solar energy can be used in many devices like space heating, drying through direct radiations and power generation etc. Air heater is an important device of solar energy. Air heater easy to create and set up, still, due to the high need of solar energy, solar air heaters performance decays with the absence of direct solar radiations. Many of researchers work had been led to cope with the availability of solar energy. Taki et al. [3] studied solar air heater both theoretically and experimentally to analyze the effects of the various parameters, like temperature, solar intensity, and airflow rate on the performance of a flat plate solar air heater. The result reviewed that black painting the back of absorber plate could increase efficiency up to 10%. Badescu [4] preceded a search on Solar air heater (SAH) to check the optimal orientation effects. The results shown that better performances came with the south, southeast and south-west locations and optimal tilt was a function of location. Fatih et al. [5] discovered that increase in heat transfer area improved the thermal efficiencies of (SAH). Singh et al. [6] completed study on baffled and flat plate solar air collectors. The study confirmed that baffled solar air collectors were 16-21% more thermally efficient due to increased flow trail of air. Ammari [7] built up a numerical model to decide the warm presentation of the brace solar air heater. It was anticipated that the brace solar air heater has improved warm execution when contrasted with that of most normal sort radiators . Bouadila et al. [8] directed an exploratory investigation to assess the warm exhibition of a solitary solar pass air heater based air radiator containing a capacity medium as a stuffed bed in a circular case. Spiral tube is considered as efficient modification regarding better heat transfer performance [9]. Graphene nanoplatelets based solar systems are also of possible use [10-11]. Goodarzi et al. [12] told that the

corrugated tube heat exchanger as effective source for heat delivery in solar collectors. The regular energy and exergy efficiencies stayed among 32-45% and 13-25% respectively. Belmonte et al. [13] completed a reenacted investigation on sun powered air frameworks with Phase Changing Material (PCM) fluidized beds to upgrade warm vitality stockpiling limit. The results obtained showed that 5000 kg PCM combined with 20 m^2 zone could meet 20-25% heating supplies in different zones in Spain. Kalaiarasi et al. [14] made an experimental study to explore thermal efficiencies of conventional Solar air heater and integrated sensible heat storage SAH . It was concluded that integrated sensible heat storage solar air heater is more efficient. Olia et al. [15] uncovered the nanofluids as the potential wellspring of warmth move in sun oriented trough. The format of solar collector do an important role in deciding the required parameters [16]. Kabeel et al. [17] conducted a full review of SAHs. It was noted that finned baffle and artificially roughened setups caused in better thermal efficiencies. In addition, Ni-Sn coated solar air heaters provided 29.73% higher yearly every day efficiency as linked to black SAH. Sarafraz et al. [18] made a few tests to show the actions of liquid metal mixture in the heat transfer co-efficient. It was reported that pressure drop and friction of the system was reduced at higher temperatures. Khadraoui et al. [19] deliberated the thermal performance of an indirect and direct solar dryer with and without latent storage unit (having, phase changing material "PCM") respectively for nocturnal usage. It was reported that direct solar dryer produced less favorable conditions in comparison to the indirect solar dryer. Moreover, Daily energy and exergy efficiency of the indirect solar dryer (ISD) touched 33.9% and 8.5% respectively. Nessim et al. [20] gave an experimental search on double pass parallel flow SAH including PCM packed in spherical capsules located in both passes. The results exposed the good thermal performance of suggested solar air heater with the daily energy efficiency of 47%. An experiment was made to forced convection solar dryer with paraffin wax as the latent heat storage unit in a separate shell and tube arrangement to dry chili by Rabha et al. [21]. It was informed that this solar dryer arrangement reduced the drying time by 122.8% in contrast with the open environment drying method. The latent heat storage used to advantage of greater energy storage density and constant temperature energy gain ensured relatively smooth energy production. In addition, latent heat storage is more effective than sensible heat storage by Sharma et al. [22] and Tyagi et al. [23]. Kabeel et al. [24] made tests on particular pass solar air heater for flat and v-corrugated absorber plate with and without PCM to check thermal performances. The result was that solar air heaters with absorber plate have higher thermal efficiencies with and without PCM as compared to that of flat plate arrangements. Pandey et al. [25] exhibited a survey on new methodologies and headway in regards to the utilization of PCMs in galaxies and inferred that no single sort of PCM is perfect for required yields. One must go on step by step to regarding usage of PCMs. Ali et al. [26] Played out a trial examination on a twofold pass sunlight based air radiator with and without capacity medium alongside Aluminum and copper bars as warm conductivity enhancer. The results were that after sunset, configurations with storage medium gives output for 1.5 and 2 hours. Krishnananth et al. [27] explored the capacity of a double pass solar air heater (DPSAH) to store the warmth with and without paraffin wax for four distinct setups and found that the effectiveness of the design having PCM containers put on the upper pass is the proficient one. A study on double pass solar air heater with a flat plate, finned plate and V-corrugated plate was made to notice the thermal performance by Sebaii et al. [28, 29]. For DPSAH with airflow from one pass to other pass kinds, PCMs never used in both passes at the same time. In addition, Alam et al. [30] presented a review on enriched heat transfer methods in DPSAHs and discovered that DPSAHs are 10-15% more effective as compared to single pass SAHs. Ozgen et al. and Chii et al. [31] performed a study on wire mesh packed DPSAH with recycling from lower pass to strengthen convective heat transfer coefficient due to increase turbulence. Ravi et al. [32] explored the double pass solar air heater with artificial roughened absorber plate in grouping with staggered ribs and multi V-shaped for Reynold number reaching from 2000 to 20000. Thermal and hydraulic efficiencies produced enhanced results. 3-D numerical simulation was conducted on solar air heater fitted with winglet vortex generator with Reynold Number reaching from 3500 to 16000 by Chamoli et al. [33]. The study showed noticeable development in convective heat transfer rate due to turbulent flow. Rajaseenivasan et al. [34] utilized two single pass SAHs with and without tabulators. The results show that system efficiency was directly proportional to Reynold number and the number of tabulators on the absorber plate. Chen et al. [35], in addition to Rehman et al. [36-37], carried out a review on progress regarding PCMs embedded in metallic foams and discovered that embedded PCMs within metallic foams could dominate the low conductivity characteristic. Also, Zhao et al. [38] came with numerical and

experimental search on heat transfer enhancement of PCM embedded with metallic foam. Numerically predicted data agreed with experimental results. It was told that embedded PCMs with metallic foam might possibly enhance heat transfer rates by 3-10 times. Sebaii et al. [39] performed studies on single pass solar air heater to revel the effect of different types of coatings. Among five types of coatings, black paint showed lowest and Ni-Sn revealed highest daily efficiency. Fath et al. [40] performed An experimental analysis of single pass Solar air heater with and without storage medium for three different shapes, shape with the corrugated arrangement of tubes filled with TSM shown higher efficiencies as compared to others, while the air mass flow rate was variable. Many of research work has been led us to the way of development of Solar air heater with condition of storage capacity, storage medium improved heat transfer rates and total thermal concerts.

The works gave us evident that DPSAH more effective than single pass ones and average thermal efficiencies of SAH increases compared with storage mediums. The problem of lower conductivity of storage mediums tends to drop the overall efficiency; research work in this subject is being performed by maintaining contact of storage mediums with resources of higher conductivity similar to Copper and Aluminum. Also the usage of paraffin wax it can be solve the issue of lower conductivity of storage mediums. Presently, main phase change material could be responded to the level storage capacity of SAHs on ether hand the lower conductivity issue could have tackled by continuing contact with higher conductivity materials. Aluminum tubes, copper rods are used in the present study not just to improve heat transfer rate in this set up, but also take benefit of high latent heats which will be very helpful in constant heat outputs during cloudy weather and after sunset.

EXPERIMENTAL SET-UP

For this experimental setup, three double pass solar air heaters was manufactured using ten tubes of aluminum (fig.1). Table 1 shows the general specifications of solar air heater (SAH). Table 2 shows General properties of aluminum. Glass wool was used to insulate the sides and the bottom base with a thickness of 25 mm (fig.2).

Figure 1. Three double pass SAH were fabricated using ten tubes of aluminum.

Table 1. General specifications of SAH.

No	parameters	Specifications
1	Dimensions	760 × 550 × 250 mm^3
2	Absorber plate	Copper 3 mm thick
3	Tubes	Material = Aluminum Length = 625 mm Outer diameter = 54 mm Inner diameter = 49 mm No. of tubes = 10
4	Thermal storage medium	Paraffin wax Th. Cond. = 0.25 W/m.K (25 ^oC) Melting point = 58 ^oC Weight/ copper tube = 0.92 kg
5	Top cover	Window glass 4 mm thick
6	Side and bottom insulation	25 mm thickness glass wool
7	Rods	Material = copper Al Th. Cond. = 205 W/m.K (25 ^oC) Length = 600 mm Diameter = 25 mm No. of rods = 5 each

Table 2. General properties of aluminum (A6061).

A6061	
Physical properties	
Density	2.70 g/cm^3 [1]
Mechanical properties	
Young's modulus (E)	68.9 GPa (9,990 ksi)
Tensile strength	124-290 MPa (18.0-42.1 ksi)
Elongation at break	12-25 %
Poisson's ratio	0.33
Thermal properties	
Melting temperature	585 ^oC (1,085 ^oF)
Thermal conductivity	151-202 W/m.K
Linear thermal expansion coefficient	2.32 × 10^{-5} K^{-1}
Specific heat capacity	897 J/kg.K
Electrical properties	
Volume resistivity	32.5-39.2 nOhm.m

Figure 2. Insulate the sides and the bottom base with a thickness of 25 mm.

The heater top surface was covered by glass window of 5 mm to obtain the solar radiation required and copper absorber plate was used to decrease the losses from convection. For the phase change material (TSM) integration, five tubes of Aluminum was utilized. For the first configurations it was filled by paraffin wax (PW), figure (3).

Figure 3. Aluminum tube filled by paraffin wax

For the second configurations, the paraffin wax was poured into the tubes after melting. For maximum absorption of solar radiation, the Aluminum tubes and the absorber plate were painted black. Copper rods were fitted in the tubes center along with the melted PW, figure (4).

Figure 4. Copper rods inside wax-immersed aluminum tubes.

Outlet and inlet conical connections was provided for the heater and to extract the heated air, an exhaust fan was provided at the outlet. The pyranometer (TBQ type) was used which have 280-3000 nm spectral range and 11.36 $\mu V/W/m^2$ sensitivity. The monitoring system of the solar radiation was connected to the pyranometer which have 1 W/m^2 resolution and 0-2000 W/m^2 range, figure (5). The data monitoring system LCD displays the global solar irradiance. Iraq Meteorological Department performed a Calibration for the solar monitoring system and the pyranometer within ±2%. K-type thermocouples were utilized to measure the solar air heater temperature in diverse locations.

Figure 5. Measuring devices and the fan.

These thermocouples were connected to figure (5) Experimental set digital multimeter to read the measurement of temperature. The temperature was measured at five diverse locations on the absorber plate, where the tubes were contained. One of the thermocouples was used to measure the temperature of air entering the collector; another one was used to measure the temperature of air exiting the collector. The lower glass surface temperature was also measured by another thermocouple. One of the thermocouples was located at wax and the Copper rod center by making a hole with 1 mm diameter in the rod, figure (6) to calculate the stored energy.

Figure 6. Thermocouple located at the center of copper rod.

Experiments were conducted on double pass solar air heater for three different configurations. Two successive days measuring were read for each of the configuration studied. The reading was taken from 9 a.m. till 8 p.m. the heater was placed facing south with 33° slope (local latitude of Baghdad, Iraq) to receive the maximum solar radiation. Figure (7) (a) and (b) shows the schematic diagram of the solar air heater and the thermocouples locations, respectively.

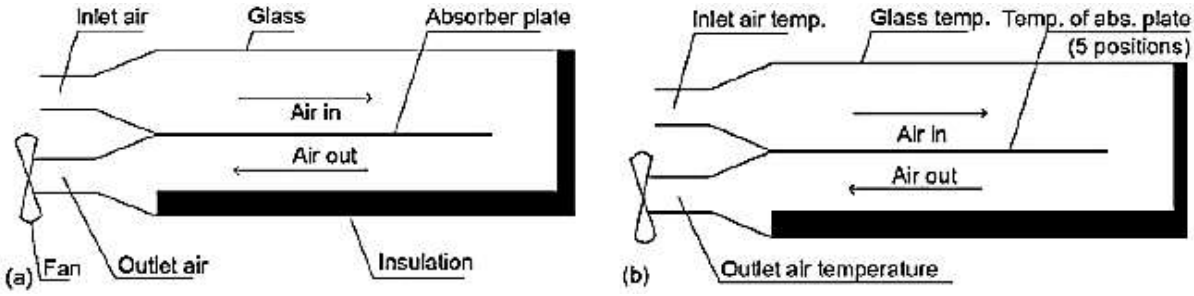

Figure 7. (a) Schematic of double pass SAH, (b) Thermocouples locations.

Threaded end caps were made for the copper tubes to close at both of their ends to prevent the PW from leaking. The velocity of air exiting through the exhaust fan was measured by anemometer, the anemometer have ±1% accuracy and 0.1 m/s resolution. The velocity then was used to calculate the flow rate.

NUMERICAL SET UP

Computational fluid dynamics was used to validate the experimental work of the solar air heater. The experimental set up geometry was modeled using Solidworks, figure (8). Ansys Workbench was used for performing the meshing process, Ansys Fluent was used for the simulations process. Figure (9) shows the mesh of the geometry, (322794) elements and (79562) nodes was generated from the meshing process. two cell zone conditions was set for the numerical work, the pipes inside the duct was set as solid body generate heat , and the rest of the duct was set as air fluid . For the boundary conditions, the inlet of the duct was set as mass air inlet flow (0.0170031 kg/s) and the outlet of the duct was set as default outlet pressure. The temperature was determined for the inlet air and the top surface of the duct were the solar flux was applied, as well as for the internal pipes of the duct. k-epsilon turbulent model was applied. The simulation was performed as steady state with 10250 iterations.

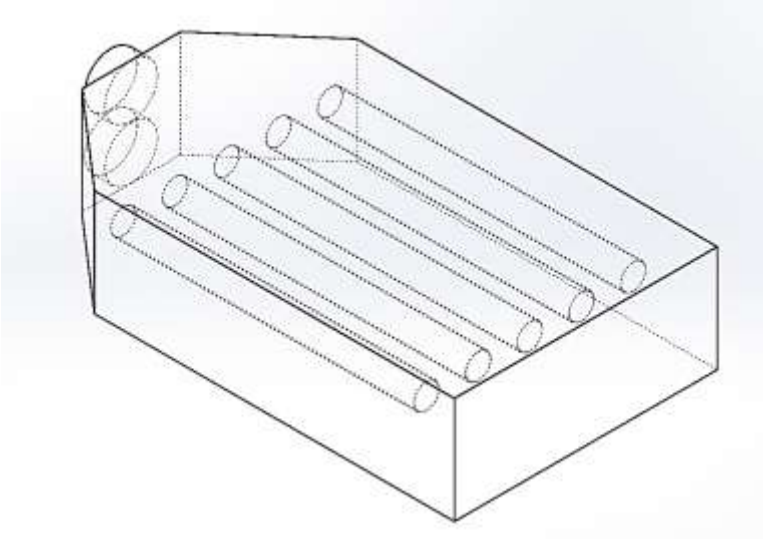

Figure 8. Geometry of the solar air heater.

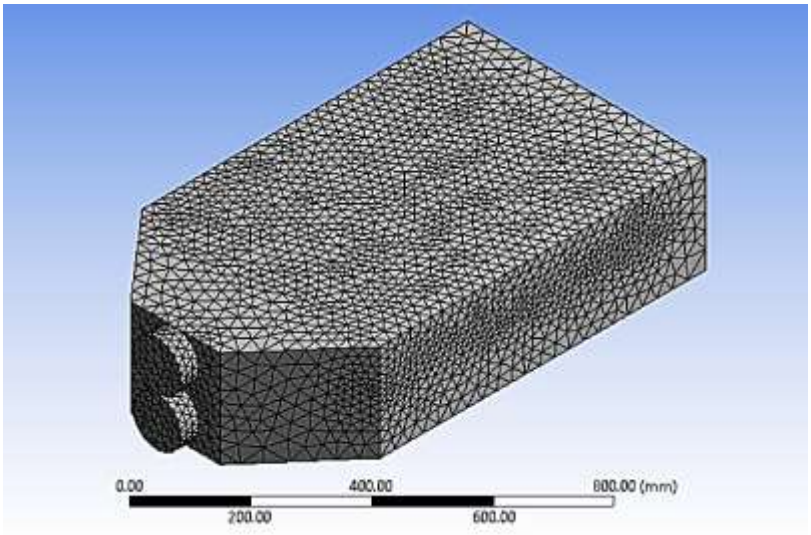

Figure 9. Mesh of the geometry model.

RESULTS AND DISCUSSION

The experimental study is conducted on three different configurations as previously mentioned. The primary parameter of importance in this experimental study is temperature measurements recorded and noted. Other

parameters which are equally important as primary parameters are derived using mathematical relations like heat input, output and storage. To understand the variability range limit we need to consider dependent and independent parameters of assessment. There is high variability in parameters of assessment like solar radiations and parameters which are direct functions of solar radiations while there will be less variability in parameters which are also functions of storage mediums for example temperature rise. For first two configurations, the experimental data is recorded from 9:00 am. to 8:00 p.m. While, for the third configuration, the data is recorded from 9:00 a.m. to 9:00 p.m. (12 h).

Figure 10, 11, 12 provides average ambient, absorber plate and temperature rise temperature data for first, second and third configurations as a function of time. Ambient temperatures were highest for third configuration and followed by lower and lowest by second and first configurations respectively. While variations in experimental data points are approximately in a similar manner for first and third configurations, on the other hand, higher standard deviations in the second configuration are due to the intermittent sky. It is evident from results that for first configuration (without PCM) higher temperatures are obtained around noon while for second configuration, temperatures are obtained higher around 10:00 a.m. in the morning, for period around noon these temperatures are lower than the first configuration due to fewer radiations reaching earth's surface caused by intermittent nature (Cloudy Day). However, these temperatures are higher around sunset due to stored energy in the second configuration. For third configuration, the day is ideal. But, higher temperatures of absorber plate are obtained around 2:00 p.m. as energy is being stored at higher rates in thermal storage medium before this time. After this, third configuration absorber plate temperatures are highest in comparison to other configurations.

This is because energy in the air is not only being drawn from the absorber plate but also thermal storage mediums. Moreover, for the first configuration solar radiations were reaching to experimental set up without hindrance due to clear sky that is why the variance in data points is almost similar throughout the day. On the other hand, for second and third configurations storage also contributes to a reduction in the variance of gathered data. At the start of the day, the temperature rise is higher for the first configuration as compared to that of others even without any thermal storage medium up to 9:30 a.m. The reason for this behavior is that in other configurations, energy is not only being transferred to air but also getting stored in thermal storage mediums. While the second configuration shows ups and downs in temperature rise values due to intermittent nature from 9:30 a.m. to around 1:30 p.m. After this time, higher temperature rise values are obtained until the end of experimentation (Clear Sky). While the third configuration shows higher temperature rise values after 9:30 a.m. in comparison to other configurations. Moreover, the temperature rise is available up to 5:30 p.m., 7:30 p.m. and 8:30 p.m. for first, second and third configurations respectively.

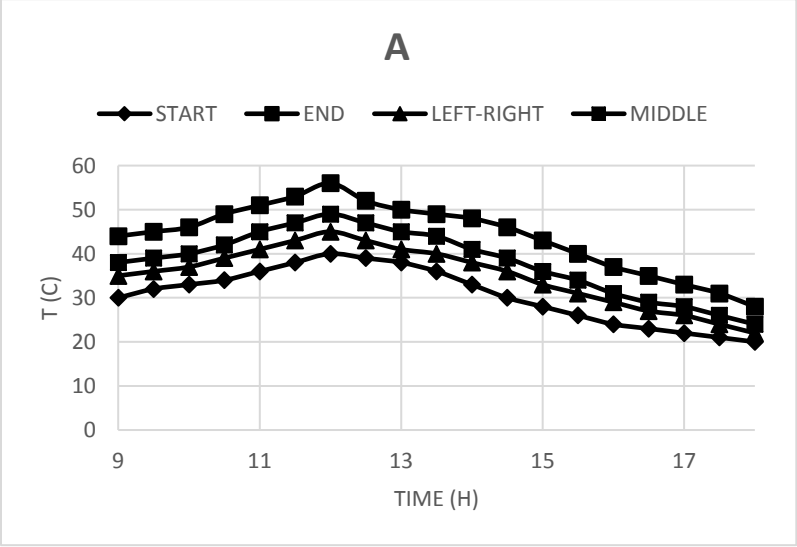

Figure 10. Temperature variation from 9 am to 6 pm for the first used configuration.

The typical different temperatures variation for the second configurations of solar air heater is shown in figure (11). The pattern of variation was the same for all configurations. All the measured temperatures were fluctuating with the intensity of solar radiation. The maximum temperature for the glass and the absorber plate was reached during noon. The temperature of exit air closely diverse with the temperature of capsule surface. The temperature of exit air touched 50 ^{o}C around noon which represent its maximum value at that point. All the temperatures experienced an appreciable rise after 8 AM , and All the temperatures experienced an appreciable decrease after 5 PM. Figure (12) shows the temperature for the third configuration used in this study.

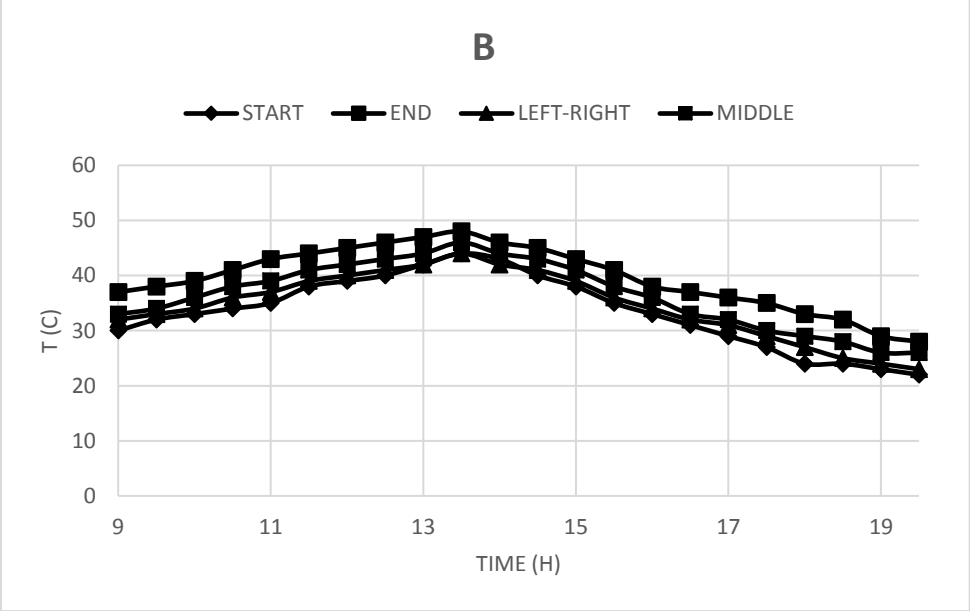

Figure 11. Temperature during the day for the three used configurations.

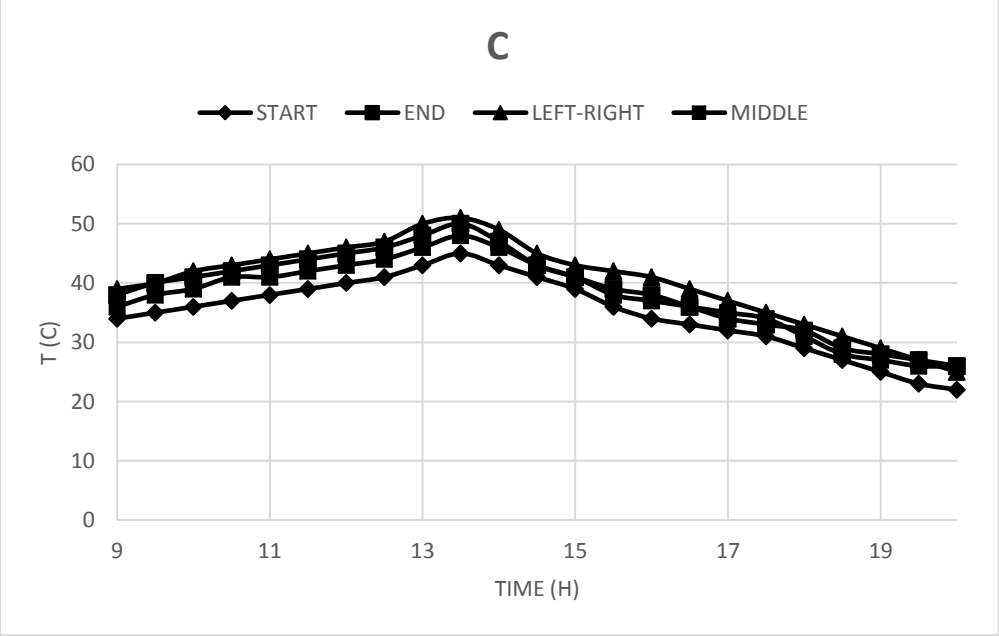

Figure 12. Temperature during the day for the three used configurations.

The graphs for solar flux will be shown and discussed for analysis. Figure 13 shows the solar flux variation for all the configurations experimented. During the first configuration, solar flux varied from 700 to 1100 W/m^2, and then decrease around noon. The potential increase in the green energy should consider these factors on serious mater. Though, during the second configuration, the solar flux was ranged from 700 to 1189 W/m^2. The solar flux for all the studied configurations was nearly equal to zero after 6 pm. The variation was not that much for the solar flux in all the studied configurations. Through the second configurations, the PW did not melted despite the high temperature that was recorded for the exit air.

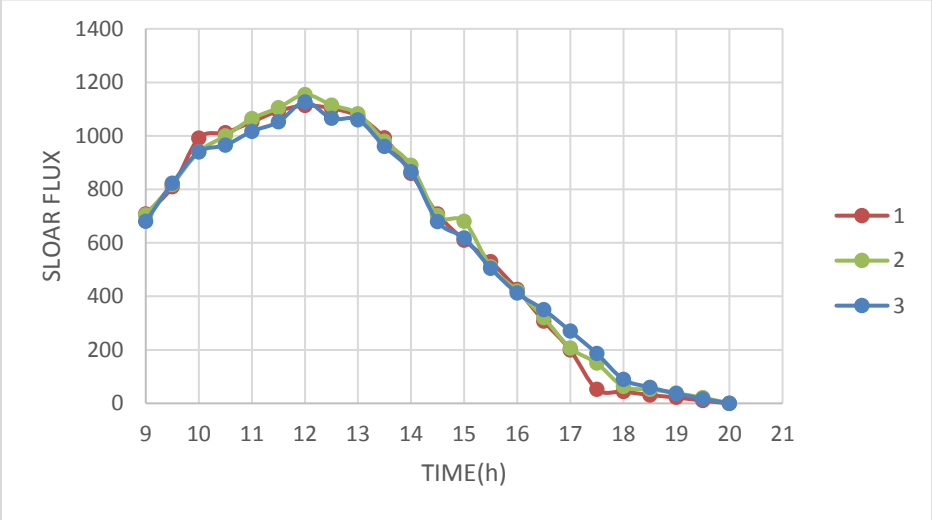

Figure 13. Solar flux variation as a function of time for all configurations.

Figures 14 shows the temperature difference (ΔT=Tout−Tin) hourly variations at the same mass flow rate. As anticipated, in the morning the ΔT increases, at noon reach its highest value, in the afternoon start to reduce. For the second and third configurations the temperature difference reach a steady value almost form 11:30 pm to 02:30 pm, then start to decrease. The first configurations keeps on rising until it reaches its peak value at 12:30 which was 12.5 °C then decreased.

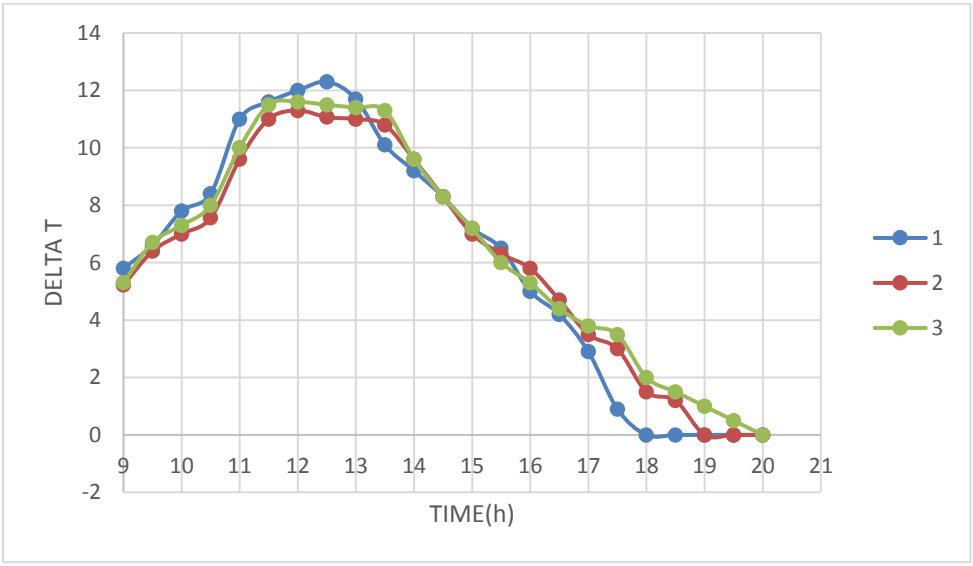

Figure 14. Temperature difference (outlet minus inlet) as a function of time for all configurations.

In the last set of experimentation Figure 15, melting of paraffin wax was achieved by storing only all of the incident energy during the daytime while utilizing the same after sunset using fan. Paraffin wax melting was done easily at 2 pm since there were no heat transfers available without the cold air outside. With this experiments set a very useful data were found. The temperature of the daytime in Iraq ranges among 15 and 26 °C during winter times and a much higher values during summer times which make it the best. All the daytime stored energy can professionally be stored and consequently used during the evening times. After the sunset, 2.5 h useful heat was gained. This can significantly reduce the equipment overall cost. It was establish that the valuable energy increased with the solar energy value, at the same mass flow rate.

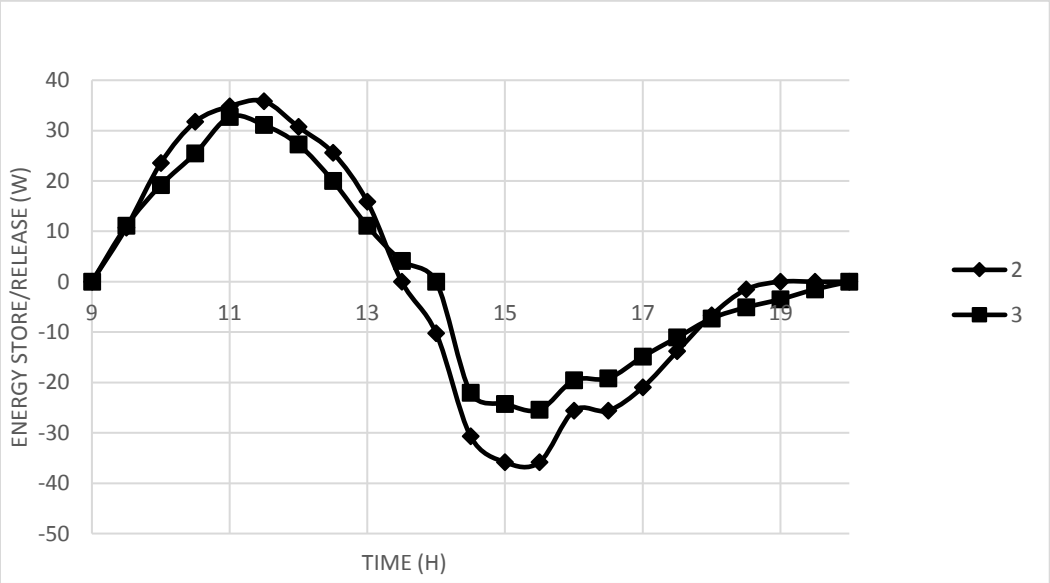

Figure 15. Energy stored over time.

The energy percentage for the first, second, and third configurations are shown in figure 16. The third configuration got the higher percentage of energy followed by the second configuration since the heat transfer was better, which was explained already. Though generally the percentage of energy increased for all the studied configurations as the time passes, since the losses of radiation during the afternoon are minimum. The third configuration got the maximum percentage of energy, which was 100 % at 7:30 pm. There was not much variation in the energy percentage as well as the capacity of storage for all the studied configurations, which shows that the energy percentage do not effected significantly with copper and paraffin wax increasing. Therefore using the second configurations can reduce the system overall cost.

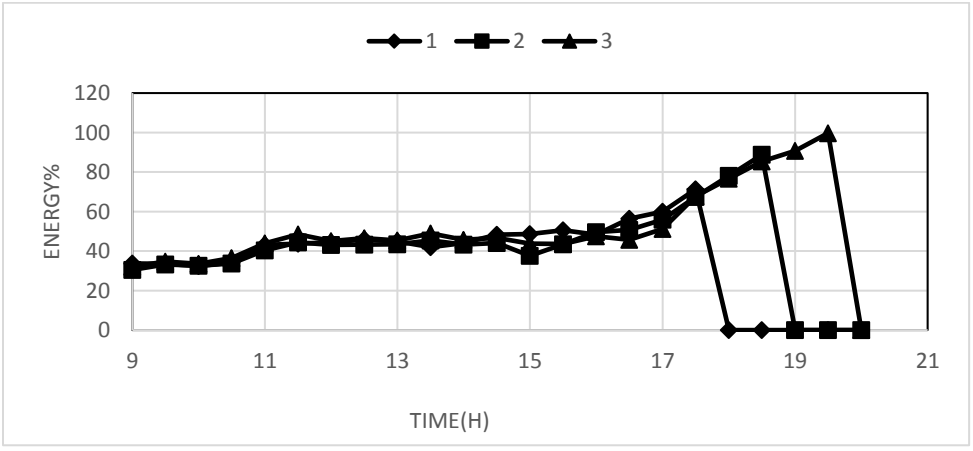

Figure 16. Percentage of energy generated from the three used configurations.

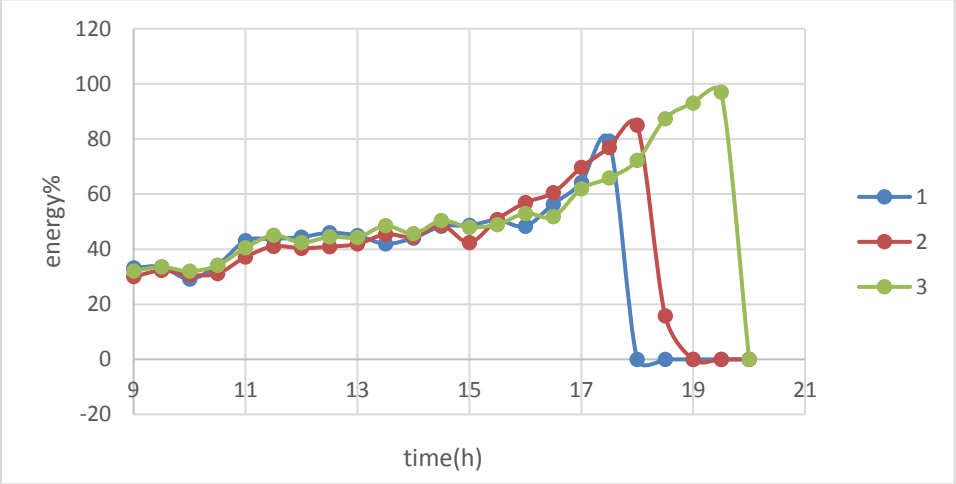

Figure 17. Percentage of energy generated from the three used configurations.

The distribution of air temperature through the solar air heater are represented in figure 18. The numerical results illustrated that the second and the first path of the collector experience an increase in the temperature of air, as a result from the energy exchanged between the airflow and the double absorbent surfaces. The direction of the flow seems to change at the end of first path which generate vortices that increase the interchange of energy for the air flow and the upper absorbent surface if compared with traditional heater, figure 19. Further, the temperature of outlet air decreased as the air flow increased in the collector since the exchange of convection would be low, Figure 19 shows the velocity stream lines for the collector. Figure 18 the distribution of air temperature through the solar air heater for a plane located at the middle of the internal tubes, which filled with paraffin wax as a latent energy storage of the charging period, at solar irradiance of 293.997 W/m^2 and fixed air mass flowrate of 0.0170031 kg/s.

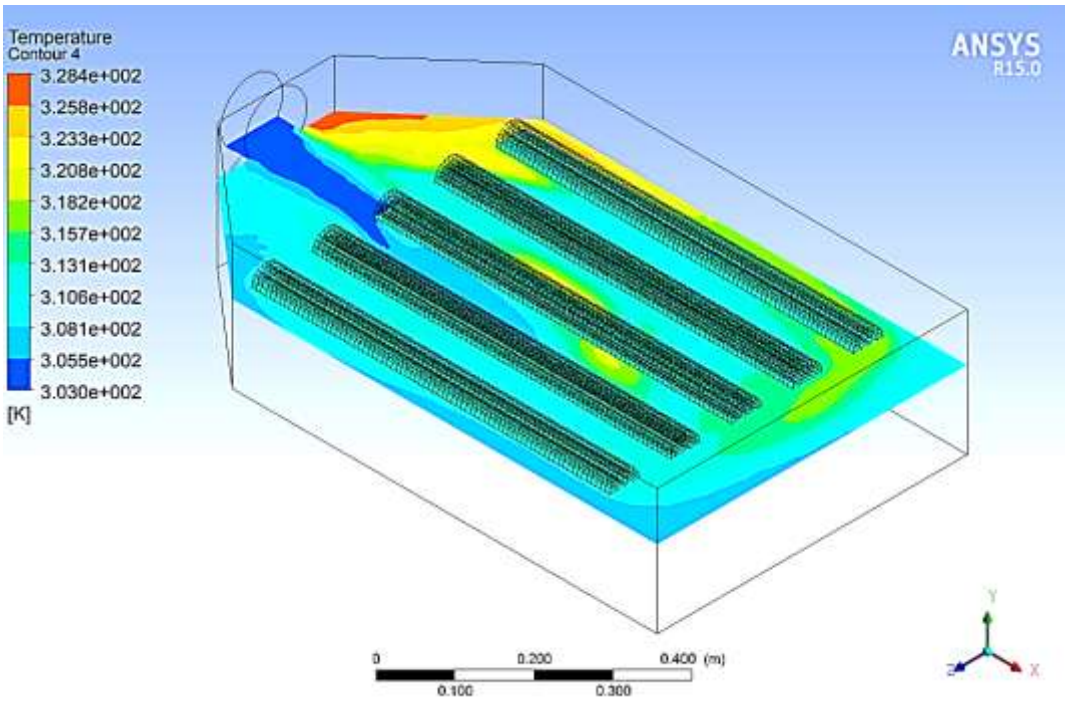

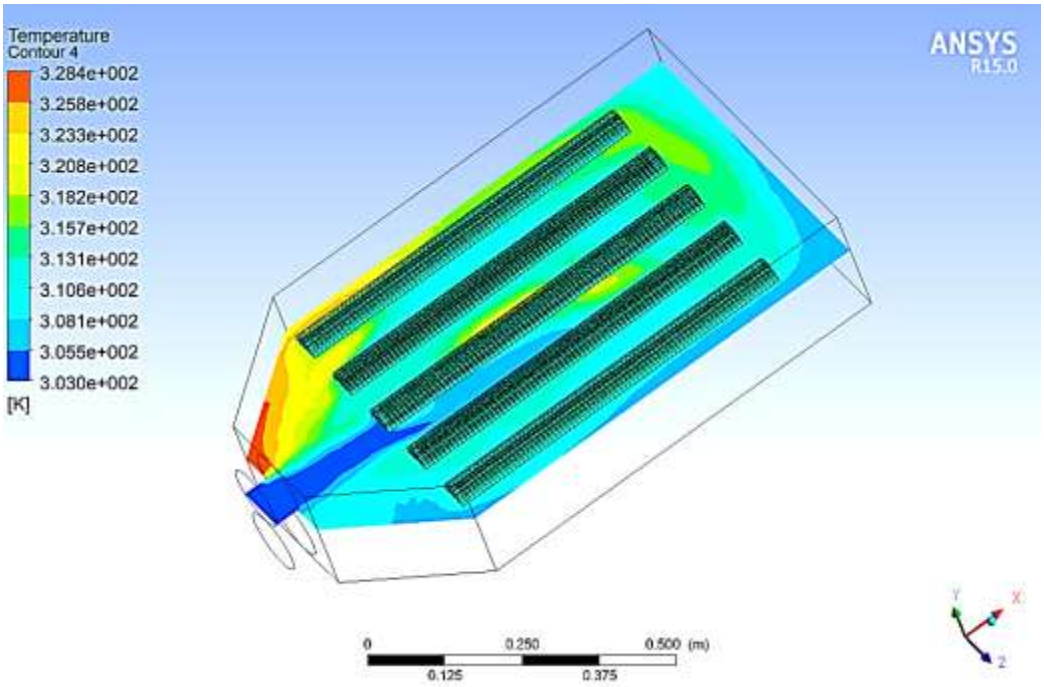

Figure 18. Temperature distribution in the collector.

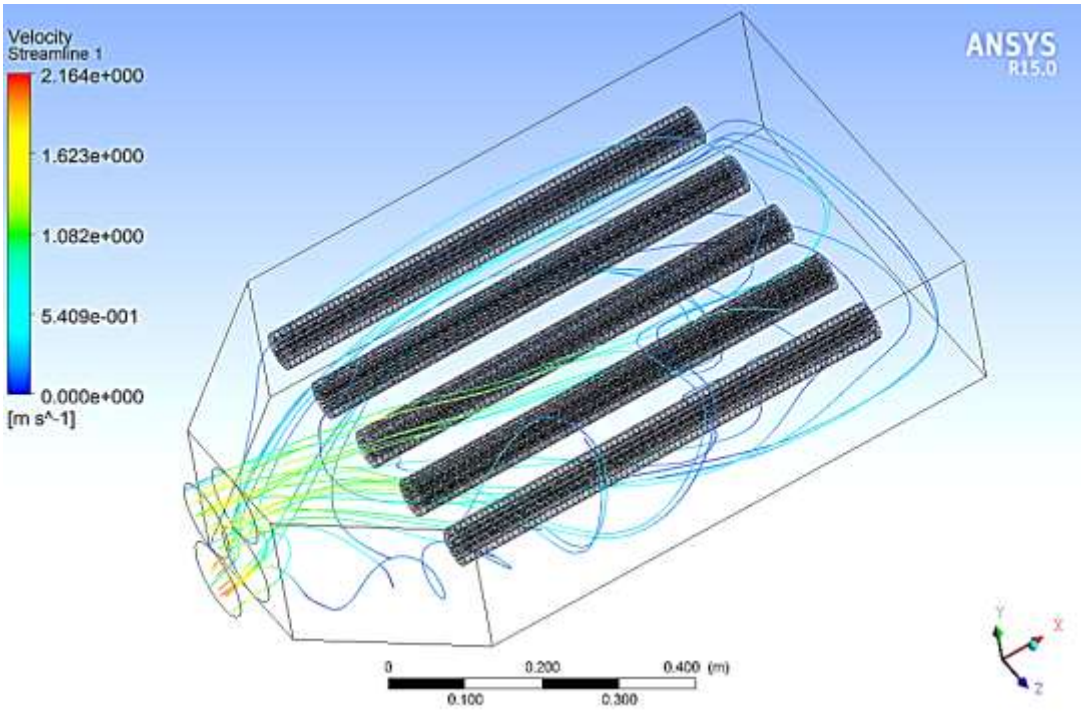

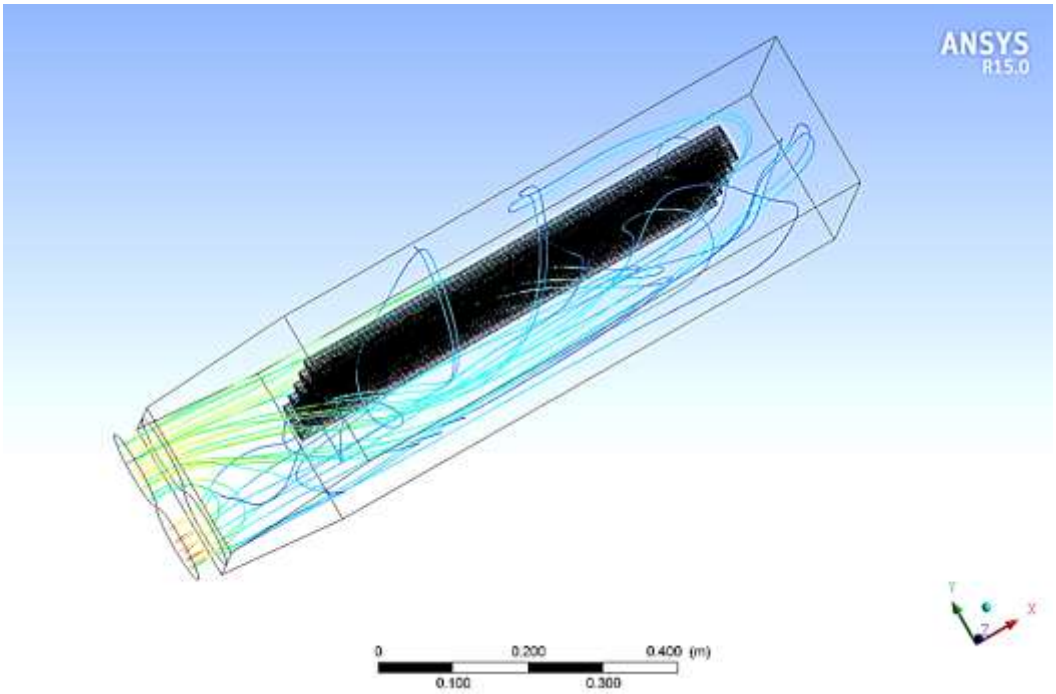

Figure 19. Velocity streamlines.

CONCLUSION

The performance of the double pass solar air heater was investigated experimentally and numerically using computational fluid dynamics. In these experimental investigations, three double pass solar air heaters was fabricated using ten tubes of aluminum. Three configurations types were used for the experiments. The experiments time lasted from 9 am to 6 pm. The results showed that:

1- For the first used configurations, the temperature start to increase as the time raises from 9 am to the noon around 12 pm then start to decrease.

2- For the second and third configurations the temperature start to increase as the time raises from 9 am to the noon around 14 pm then start to decrease.

3- For the three used configurations, the solar flux start to increase as the time raises from 9 am to the noon around 12 pm then start to decrease.

4- For the three used configurations , the energy percent keeps raising form 9 am then as the sunset the energy falls to zero starting with the first configurations and ending with the third configurations.

5- The numerical work showed that the air velocity create vortices in the collector.

REFERENCES

[1] M.M. Sarafraz, I. Tlili, Z. Tian, M. Bakouri, M.R. Safae, "Smart optimization of a thermosyphon heat pipe for an evacuated tube solar collector using response surface methodology (RSM)", *Physica A: Statistical Mechanics and its Applications*, Vol. 534, Pp. 122146, 2019.

[2] M.R. Safaei, H.R. Goshayeshi, and I. Chaer, "Solar Still Efficiency Enhancement by Using Graphene Oxide/Paraffin Nano-PCM", *Energies*, Vol. 12, No. 10, Pp. 2002, 2019.

[3] M.T. Al-Kamil, and A. Al-Ghareeb, "Effect of thermal radiation inside solar air heaters", *Energy conversion and management*, Vol. 38 (14), Pp. 1451-1458, 1997.

[4] V. Bădescu, "The dependence of solar air heater performance upon tilt and orientation", *Energy conversion and management*, Vol. 30, No. 2, Pp. 179-185, 1990.

[5] F. Bayrak, and H.F. Oztop, "Experimental analysis of thermal performance of solar air collectors with aluminum foam obstacles", *Isi Bilimi Ve Teknigi Dergisi-Journal Of Thermal Science And Technology*, Vol. 35, No. 1, Pp. 11-20, 2015.

[6] V. Singh, A. Singh, and A. Verma, "Experimental Investigation of Double Pass Solar Air Heater with Baffled Absorber Plate", 2017.

[7] H. Ammari, "A mathematical model of thermal performance of a solar air heater with slats", *Renewable Energy*, Vol. 28, No. 10, Pp. 1597-1615, 2003.

[8] S. Bouadila, S. Kooli, M. Lazaar, S. Skouri, and A. Farhat, "Performance of a new solar air heater with packed bed latent storage energy for nocturnal use", *Applied Energy*, Vol. 110, Pp. 267-275, 2013.

[9] M. Bahiraei, H.K. Salmi, and M.R. Safaei, "Effect of employing a new biological nanofluid containing functionalized graphene Nano platelets on thermal and hydraulic characteristics of a spiral heat exchanger", Energy conversion and management, Vol. 180, Pp. 72-82, 2019.

[10] M.M. Sarafraz, I. Tlili, Z. Tian, M. Bakouri, M.R. Safaei, and M. Goodarzi, "Thermal evaluation of graphene nanoplatelets nanofluid in a fast-responding HP with the potential use in solar systems in smart cities", Applied Sciences, 9 (10), Pp. 2101, 2019.

[11] M.M. Sarafraz, M.R. Safaei, Z. Tian, M. Goodarzi, E.P.B. Filho, and M. Arjomandi, "Thermal Assessment of Nano-Particulate Graphene- Water/Ethylene Glycol (WEG 60: 40) Nano-Suspension in a Compact Heat Exchanger", *Energies*, 12 (10), Pp. 1929, 2019.

[12] M. Goodarzi, A. Amiri, M.S. Goodarzi, M.R. Safaei, A. Karimipour, E.M. Languri, M. Dahari, "Investigation of heat transfer and pressure drop of a counter flow corrugated plate heat exchanger using MWCNT based nanofluids", *International communications in heat and mass transfer*, Vol. 66, Pp. 172-179, 2015.

[13] J. Belmonte, "Air-based solar systems for building heating with PCM fluidized bed energy storage", *Energy and Buildings*, Vol. 130, Pp. 150-165, 2016.

[14] G. Kalaiarasi, R. Velraj, and M.V. Swami, "Experimental energy and exergy analysis of a flat plate solar air heater with a new design of integrated sensible heat storage", *Energy*, Vol. 111, Pp. 609-619, 2016.

[15] H. Olia, M. Torabi, M. Bahiraei, M.H. Ahmadi, M. Goodarzi, and M.R. Safaei, "Application of nanofluids in thermal performance enhancement of parabolic trough solar collector: state-of-the-art", *Applied Sciences*, Vol. 9, No. 3, Pp. 463, 2019.

[16] H.R. Goshayeshi, and M.R. Safaei, "Effect of absorber plate surface shape and glass cover inclination angle on the performance of a passive solar still" *International Journal of Numerical Methods for Heat & Fluid Flow*, 2019.

[17] A.E. Kabeel, M.H. Hamed, Z.M. Omara, A.W. Kandeal, "Solar air heaters: Design configurations, improvement methods and applications–A detailed review", *Renewable and Sustainable Energy Reviews*, Vol. 70, Pp. 1189-1206, 2017.

[18] M.M. Sarafraz, M.R. Safaei, M. Goodarzi, B. Yang, M. Arjomandi, "Heat transfer analysis of Ga-In-Sn in a compact heat exchanger equipped with straight micro-passages", *International Journal of Heat and Mass Transfer*, Vol. 139, Pp. 675-684, 2019.

[19] A.E. Khadraoui, S. Bouadila, S. Kooli, and A.F.A. Guizani, "Thermal behavior of indirect solar dryer: Nocturnal usage of solar air collector with PCM", *Journal of cleaner production*, Vol. 148, Pp. 37- 48, 2017.

[20] N. Arfaoui, S. Bouadila, and A. Guizani, "A highly efficient solution of off-sunshine solar air heating using two packed beds of latent storage energy", *Solar Energy,* Vol. 155, Pp. 1243-1253, 2017.

[21] D. Rabha, and P. Muthukumar, "Performance studies on a forced convection solar dryer integrated with a paraffin wax–based latent heat storage system", *Solar Energy,* Vol. 149, Pp. 214-226, 2017.

[22] A. Sharma, V.V. Tyagi, C.R. Chen, and D. Buddhi, "Review on thermal energy storage with phase change materials and applications", *Renewable and Sustainable energy reviews,* 13 (2), Pp. 318-345, 2009.

[23] V.V. Tyagi, N.L. Panwar, N.A. Rahim, R. Kothari, "Review on solar air heating system with and without thermal energy storage system", *Renewable and Sustainable Energy Reviews,* Vol. 16, No. 4, Pp. 2289-2303, 2012.

[24] A.E. Kabeel, A. Khalil, S.M. Shalaby, and M.E. Zaye, "Experimental investigation of thermal performance of flat and v- corrugated plate solar air heaters with and without PCM as thermal energy storage", *Energy Conversion and Management*, Vol. 113, Pp. 264-272, 2016.

[25] A.K. Pandey, M.S. Hossain, V.V. Tyagi, N.A. Rahim, J. Selvaraj, A. Sari, "Novel approaches and recent developments on potential applications of phase change materials in solar energy", *Renewable and Sustainable Energy Reviews,* Vol. 82, Pp. 281-323, 2018.

[26] H.M. Ali, A.I. Bhatti, and M. Ali, "An experimental investigation of performance of a double pass solar air heater with thermal storage medium", *Thermal Science*, Vol. 19, No. 5, Pp. 1699-1708, 2015.

[27] S. Krishnananth, and K.K. Murugavel, "Experimental study on double pass solar air heater with thermal energy storage", Journal *of King Saud University- Engineering Sciences,* 25 (2), Pp. 135-140, 2013.

[28] A. El-Sebaii, "Thermal performance investigation of double pass-finned plate solar air heater," *Applied Energy*, Vol. 88, No. 5, Pp. 1727-1739, 2011.

[29] A.A. El-Sebaiia, S. Aboul-Enein, M.R.I. Ramadan, S.M. Shalaby, and B.M. Moharram, "Investigation of thermal performance of-double pass-flat and v-corrugated plate solar air heaters", *Energy,* Vol. 36, No. 2, Pp. 1076-1086, 2011.

[30] T. Alam, and M.H. Kim, "Performance improvement of double-pass solar air heater–A state of art of review", *Renewable and Sustainable Energy Reviews,* Vol. 79, Pp. 779-793, 2017.

[31] C.D. Ho, H. Chang, C.S. Lin, C.C. Chao, and Y.E. Tien, "Analytical and experimental studies of wire mesh packed double-pass solar air heaters under recycling operation", *Energy Procedia,* Vol. 75, Pp. 403-409, 2015.

[32] R.K. Ravi, and R. Saini, "Experimental investigation on performance of a double pass artificial roughened solar air heater duct having roughness elements of the combination of discrete multi V shaped and staggered ribs", *Energy*, Vol. 116, Pp. 507-516, 2016.

[33] S. Chamoli, R. Lu, D. Xu, P. Yu, "Thermal performance improvement of a solar air heater fitted with winglet vortex generators", *Solar Energy,* 2018. 159: p. 966-983, 2018.

[34] T. Rajaseenivasan, S. Srinivasan, and K. Srithar, "Comprehensive study on solar air heater with circular and V-type turbulators attached on absorber plate", Energy, 88, Pp. 863-873, 2015.

[35] J. Chen, D. Yang, J. Jiang, A. Ma, and D. Song, "Research progress of phase change materials (PCMs) embedded with metal foam (a review)", *Procedia Materials Science*, 4, Pp. 389-394, 2014.

[36] T. Rehman, H.M. Ali, M.M. Janjua, U. Sajjad, and W.M. Yan, "A critical review on heat transfer augmentation of phase change materials embedded with porous materials/foams", *International Journal of Heat and Mass Transfer*, Vol. 135, Pp. 649-673, 2019.

[37] T. Rehman, H.M. Ali, A. Saieed, W. Pao, M. Ali, "Copper foam/PCMs based heat sinks: an experimental study for electronic cooling systems", *International Journal of Heat and Mass Transfer,* Vol. 127, Pp. 381-393, 2018.

[38] C. Zhao, W. Lu, and Y. Tian, "Heat transfer enhancement for thermal energy storage using metal foams embedded within phase change materials (PCMs)", *Solar energy*, Vol. 84, No. 8, Pp. 1402-1412, 2010.

[39] A. El-Sebaii, and H. Al-Snani, "Effect of selective coating on thermal performance of flat plate solar air heaters", Energy, Vol. 35, No. 4, Pp. 1820-1828, 2010.

[40] H.E. Fath, "Thermal performance of a simple design solar air heater with built-in thermal energy storage system", *Renewable energy,* Vol. 6, No. 8, Pp. 1033-1039, 1995.